doi:10.1093/brain/awx338 BRAIN 2018: 141; 472–485 | 472

BRAIN
A JOURNAL OF NEUROLOGY

A widespread visually-sensitive functional network relates to symptoms in essential tremor

Derek B. Archer,[1] Stephen A. Coombes,[1] Winston T. Chu,[1,2] Jae Woo Chung,[1] Roxana G. Burciu,[1] Michael S. Okun,[3] Aparna Wagle Shukla[3] and David E. Vaillancourt[1,2,3]

Essential tremor is a neurological syndrome of heterogeneous pathology and aetiology that is characterized by tremor primarily in the upper extremities. This tremor is commonly hypothesized to be driven by a single or multiple neural oscillator(s) within the cerebello-thalamo-cortical pathway. Several studies have found an association of blood-oxygen level-dependent (BOLD) signal in the cerebello-thalamo-cortical pathway with essential tremor, but there is behavioural evidence that also points to the possibility that the severity of tremor could be influenced by visual feedback. Here, we directly manipulated visual feedback during a functional MRI grip force task in patients with essential tremor and control participants, and hypothesized that an increase in visual feedback would exacerbate tremor in the 4–12 Hz range in essential tremor patients. Further, we hypothesized that this exacerbation of tremor would be associated with dysfunctional changes in BOLD signal and entropy within, and beyond, the cerebello-thalamo-cortical pathway. We found that increases in visual feedback increased tremor in the 4–12 Hz range in essential tremor patients, and this increase in tremor was associated with abnormal changes in BOLD amplitude and entropy in regions within the cerebello-thalamo-motor cortical pathway, and extended to visual and parietal areas. To determine if the tremor severity was associated with single or multiple brain region(s), we conducted a birectional stepwise multiple regression analysis, and found that a widespread functional network extending beyond the cerebello-thalamo-motor cortical pathway was associated with changes in tremor severity measured during the imaging protocol. Further, this same network was associated with clinical tremor severity measured with the Fahn, Tolosa, Marin Tremor Rating Scale, suggesting this network is clinically relevant. Since increased visual feedback also reduced force error, this network was evaluated in relation to force error but the model was not significant, indicating it is associated with force tremor but not force error. This study therefore provides new evidence that a widespread functional network is associated with the severity of tremor in patients with essential tremor measured simultaneously at the hand during functional imaging, and is also associated with the clinical severity of tremor. These findings support the idea that the severity of tremor is exacerbated by increased visual feedback, suggesting that designers of new computing technologies should consider using lower visual feedback levels to reduce tremor in essential tremor.

1 Laboratory for Rehabilitation Neuroscience, Department of Applied Physiology and Kinesiology, University of Florida, Gainesville, FL, USA
2 Department of Biomedical Engineering, University of Florida, Gainesville, FL, USA
3 Department of Neurology and Center for Movement Disorders and Neurorestoration, College of Medicine, University of Florida, Gainesville, FL, USA

Correspondence to: David E. Vaillancourt, PhD
University of Florida
Laboratory for Rehabilitation Neuroscience
Department of Applied Physiology and Kinesiology
PO Box 118205
Gainesville, FL 32611-8205, USA
E-mail: vcourt@ufl.edu

Received July 12, 2017. Revised October 2, 2017. Accepted October 21, 2017. Advance Access publication December 22, 2017

Keywords: movement disorders; tremor; cerebellar function; motor cortex; motor control

Abbreviations: BOLD = blood-oxygen level-dependent; FA_T = free-water-corrected fractional anisotropy maps; FTM-TRS = Fahn, Tolosa, Marin Tremor Rating Scale; IPL = inferior parietal lobule; M1 = primary motor cortex; MVC = maximum voluntary contraction; SPL = superior parietal lobule

Introduction

Essential tremor is a neurological syndrome of heterogeneous pathology and aetiology that is characterized by a progressive tremor primarily in the upper extremities. Although essential tremor can affect the head, voice, legs and trunk in 10–40% of cases, the upper limbs and hands are affected in at least 95% of cases (Elble, 2000; Whaley *et al.*, 2007). The tremor is commonly hypothesized to be driven by a single or multiple neural oscillator(s) within the cerebellum, thalamus, and motor cortex (Buijink *et al.*, 2015; Fang *et al.*, 2016). Both behavioural and neuroimaging experiments, however, support the hypothesis that tremor may be affected by abnormal neural processing in areas outside of these specific regions (Feys *et al.*, 2003; Keogh *et al.*, 2004; Neely *et al.*, 2015). A prior behavioural experiment demonstrated that patients with essential tremor had more tremor with eyes opened compared to eyes closed, which indicates that tremor could be driven by visual information and therefore visual areas of the brain (Gironell *et al.*, 2012). This evidence has been reinforced with a functional MRI study, which showed that hyperactive blood oxygen level-dependent (BOLD) signal in the primary visual cortex positively correlates with tremor severity (Neely *et al.*, 2015). Although this set of findings motivates the hypothesis that alterations in visual feedback could change the tremor severity, it remains unclear which brain circuits may be amplifying tremor.

It is important to understand how visual feedback influences tremor for two reasons. First, in the work setting, it is established that 15–25% of patients with essential tremor retire prematurely, and ~60% choose not to seek promotion because of increased tremor (Shalaby *et al.*, 2016). A study evaluating ~100 million worldwide job postings also found that 80% of jobs require computer skills, and therefore potential employees would be required to interact with computers and visual displays (Peng, 2017). Thus, it is crucial to better understand how and to what extent patients with essential tremor are influenced by visual display settings. Second, as people continue to use hand-held devices for mobile computing, tablets and laptops for work-place efficiency, and other novel devices, it is fundamental to better understand how the brain processes visual feedback differently in essential tremor. By understanding whether visual feedback modifies tremor, this allows for the study of the brain circuits that function abnormally in essential tremor.

This study used a functional MRI grip force task to test the hypothesis that an increase in visual feedback exacerbates tremor in essential tremor. A grip force task was used as it allows for the evaluation of the BOLD signal with a tightly controlled task without creating image artefacts as a result of large motions of the limbs (Diedrichsen and Shadmehr, 2005). Moreover, this same task has already been found to be a robust measure of tremor (Vaillancourt *et al.*, 2003). If tremor is increased acutely by increasing visual feedback, this affords an opportunity to establish a link between changes in brain function that directly relate to changes in tremor. In prior work, amplifying visual feedback in healthy adults resulted in increased BOLD signal within the inferior parietal lobule, primary motor cortex, dorsal premotor cortex, ventral premotor cortex, supplementary motor area, and extrastriate visual areas (Coombes *et al.*, 2010). If increases in visual feedback exacerbate tremor in essential tremor, we anticipate that this will be related to an altered BOLD response in the cerebellum, thalamus, and motor cortex, as well as in parietal and visual areas. Further, we examine how the change in BOLD signal relates to the change in tremor with increases in visual feedback using a birectional stepwise multiple regression analysis. If one region is the central driver of tremor, we would expect only changes in BOLD signal within this region to relate to the changes in the severity of tremor with increases in visual feedback; in contrast, if essential tremor is driven by multiple oscillators, multiple regions will be included in the multiple regression analysis. Finally, we examine if the model found to be associated with changes in the severity of tremor during this motor control task is generalizable to clinical tremor severity, and thus clinically relevant, by examining this network with the Fahn, Tolosa, Marin Tremor Rating Scale (FTM-TRS).

Materials and methods

The study included 37 participants: 19 with essential tremor and 18 control subjects. All essential tremor patients were diagnosed by a movement disorder neurologist using established criteria (Deuschl *et al.*, 1998) and tested after overnight withdrawal from anti-tremor medication. All patients were right-handed with bilateral tremor. Control subjects were right handed without clinical tremor. Tremor severity was assessed using the FTM-TRS (Table 1). Cognitive function of all participants was measured using the Montreal Cognitive Assessment (MoCA) (Table 1). Maximum voluntary contraction (MVC), sex, age, and disorder duration can be found in Table 1. All procedures were approved by the local

Table 1 Subject characteristics

Measure	Group	
	Essential tremor	Control
Sample size	19	18
Sex	(7 M/12 F)	(8 M/10 F)
MVC	50.86 (15.12)	56.83 (14.74)
Age (years)	65.74 (11.56)	63.66 (7.58)
MoCA	27.37 (2.63)	27.77 (1.40)
FTM-TRS	39.21 (20.33)*	0.55 (0.92)
Disorder duration	23.65 (19.87)	-

*$P < 0.05$. Data represent mean (standard deviation) or count.

Institutional Review Board and conducted according to the Declaration of Helsinki. Participant's provided written consent before testing.

Force data acquisition and force task

A fibre-optic force transducer was used and had a resolution of 0.025 N (Neuroimaging Solutions LLC). The force data produced by the patient were transmitted with a fibre-optic cable to a SM130 Optical Sensing Interrogator (Micron Optics), which digitized the force at 125 Hz. Custom LabVIEW software (National Instruments) converted the digitized force to Newtons.

Participants were trained on the task and the MVC was measured before scanning. Participants then completed a training session where they were instructed to maintain a contraction of maximum force for 3 s. The maximum force was averaged over three trials and used as the MVC for the experiment. During the task, participants produced 15% of their MVC by gripping the force transducer between their thumb and index finger (Fig. 1A). Participants performed two tasks (low and high visual feedback) (Fig. 1B).

Each task had two conditions: rest and force. Participant's viewed a visual display which projected the task, which consisted of two bars—one white and one red/green (Fig. 1C). The white target bar was set at 15% of each participant's MVC. The coloured bar was used to cue the participant to rest or produce force. During rest, participants were instructed to passively view the visual display. During force, the participants produced force and the green bar fluctuated around the target bar in real-time to reflect the amount of force production. Each condition lasted 30 s. Each task began and ended with a rest condition, and lasted 270 s.

Visual feedback manipulation

We manipulated visual feedback between tasks by changing the visual gain on the visual display, as this variable has been shown to effectively alter behaviour and ensures a standardized unit of measurement for easier replication (Vaillancourt *et al.*, 2006). We first calculated the difference between the amount of force produced by the subject and the target force (15% MVC). This difference was then multiplied by a visual gain factor for the low and high visual feedback conditions, which changed the spatial amplitude of visual feedback by using the following formula:

$$Cursor\ Position = (F_p - F_t) * G + F_t \quad (1)$$

in which F_P is the force produced by the subject, F_t is the target force, and G is the gain level used to manipulate the spatial amplitude of visual feedback.

The visual gain level (G) can be altered by modifying two different variables: (i) distance from the visual display; or (ii) changing the height of the force fluctuations provided to the participant on the visual display. We manipulated visual feedback by multiplying the error on the screen by a low value (low visual gain) or high value (high visual gain). We chose visual gain levels below (0.039°) and above (6.9°) 0.5° since this level has shown to be a breakpoint in visuomotor system activity (Coombes *et al.*, 2010). Figure 1D–K illustrates the visual gain manipulation. At the low visual gain level (Fig. 1D), a 1 N difference between the target bar and the force bar is represented by a small displacement on the screen such that the green bar and white bar are close to each other (Fig. 1E). By attenuating the visual error, there are very small fluctuations in the visual feedback viewed by the subject, and there is reduced spatial amplitude visual feedback on the screen, leading to greater force variability and error (control example: Fig. 1F; essential tremor example: Fig. 1G). At the high gain level (Fig. 1H), the visual angle is increased, the error is magnified, and a difference of 1 N of force between the green bar and white bar is represented by a larger spatial amplitude (Fig. 1I). There is increased spatial amplitude visual feedback, which corresponds with a decrease in force variability and error (control example: Fig. 1J; essential tremor example: Fig. 1K).

Force data analysis

Four force data measures at each visual feedback condition were calculated using MATLAB: mean force (%MVC), unfiltered force error (RMSE), RMSE low-pass filtered into the 0–3 Hz range, and sum of power of force between 4–12 Hz. We chose to evaluate force tremor between the 4–12 Hz range since this range is where a majority of the tremor is contained (Elble, 1986; Elble *et al.*, 1994; Deuschl and Elble, 2000; Neely *et al.*, 2015). The middle 25 s period of each trial was analysed to ensure that subjects had reached a constant level of force. The low and high visual feedback measures (mean force, RMSE unfiltered, RMSE 0–3 Hz, sum of power in 4–12 Hz) were subtracted to obtain a high-low difference measure (mean $Force_{H\text{-}L}$, Force Unfiltered $Error_{H\text{-}L}$, Force 0-3 Hz $Error_{H\text{-}L}$, and Force $Tremor_{H\text{-}L}$). Each measure was tested for homogeneity by conducting a Levene's test, and was followed by either an independent samples *t*-test or a Mann-Whitney U-test (significance at $P < 0.05$).

Functional MRI and T_1 data acquisition

MRI was collected using a 32-channel SENSE head coil inside a 3 T magnetic resonance scanner (Achieva). T_1-weighted images (resolution: 1 mm isotropic, repetition time = 8.2 ms, echo time = 3.7 ms, flip angle = 8°, field of view = 240 mm^3) were acquired in 170 axial slices and functional data were acquired in 55 axial slices using a single-shot gradient echo-planar imaging pulse sequence (resolution: 3 mm isotropic, repetition time = 3000 ms, echo time = 30 ms, flip angle = 90°, field of view = 240 mm^3). Each functional scan lasted 270 s.

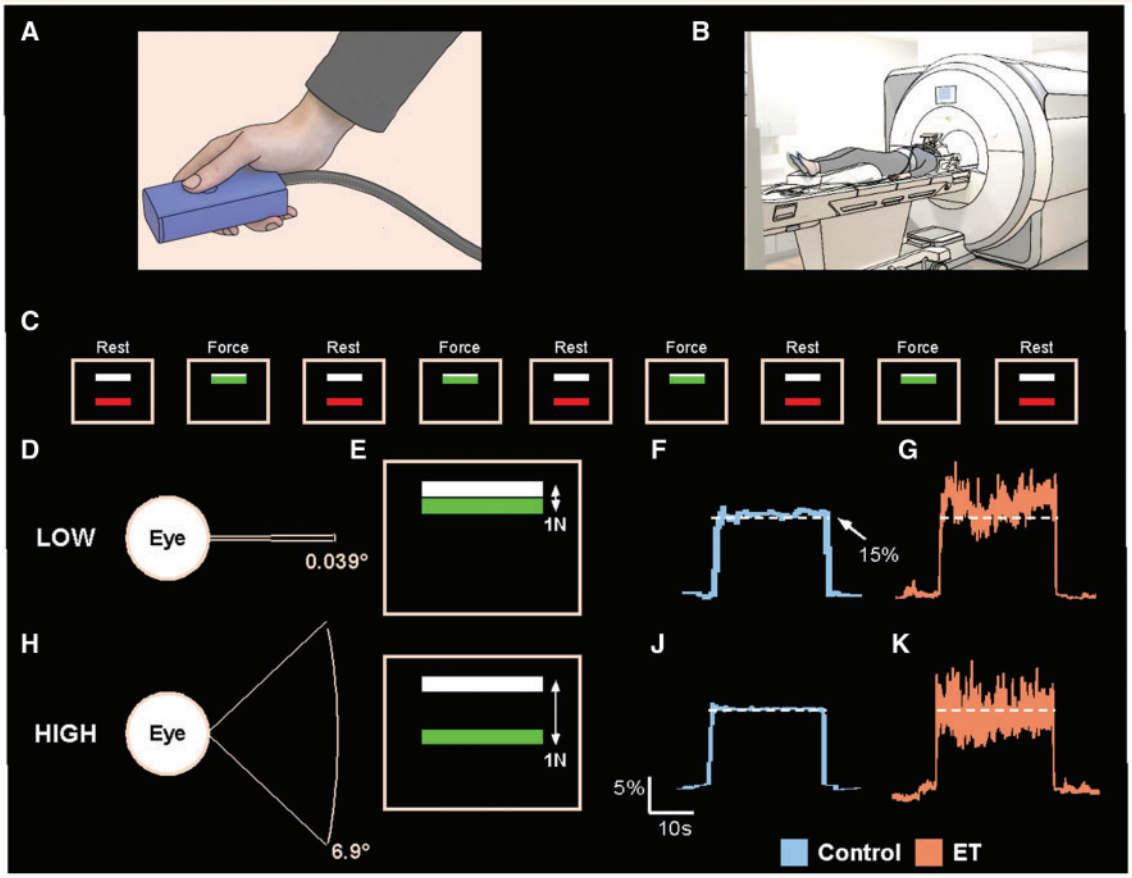

Figure 1 Experimental set-up. The force transducer was held between the thumb and the index finger by the participant during the MRI session (**A**), and the participant laid in the supine position in which the hand and transducer rested on the upper leg (**B**). Above the field of view of the participant was a mirror, which reflected the visual display. The visual display instructed the participant when to produce force. Initially, the participant rested for 30 s in the 'Rest' condition (**C**). At the end of the Rest condition, the colour of the bar would change, indicating the beginning of the 'Force' condition. The participant then began producing force for 30 s, thus fluctuating around the white target bar. At the end of the 30 s, the colour of the bar would change again, indicating the beginning of the 'Rest' condition. An example showing the visual gain manipulation (**D** and **H**), how it is perceived by the subject on the visual display (**E** and **I**), and example force traces for a control subject (**F** and **J**) and an essential tremor (ET) subject (**G** and **K**) is also shown for the low and high visual feedback conditions.

Subjects wore ear plugs to reduce scan noise and small cushions were placed around the head to reduce head motion.

Functional MRI imaging data analysis

Functional imaging data were analysed with AFNI software (Analysis of Functional NeuroImages; National Institutes of Health, Bethesda, MD), SPM8 software, SUIT toolbox of SPM8 (Diedrichsen *et al.*, 2009), and custom UNIX shell scripts. Whole-brain statistical maps were computed with AFNI; cerebellum-specific fine-tuning of the statistical maps was performed with SPM8 and SUIT. The SUIT toolbox of SPM8 is specifically designed to precisely align the cerebellum of subjects to a cerebellum template.

Whole-brain functional MRI preprocessing

The first three volumes of each functional scan were excluded to allow for equilibration of the T_1 image; remaining volumes were slice acquisition-dependent slice-time corrected. The anatomical image was then skull-stripped. The functional volumes were registered to a base volume via rigid body rotations and aligned with the anatomical image in a single transformation. For the whole-brain analysis, the functional volumes were warped into MNI space and smoothed with an 8 mm full-width at half-maximum Gaussian kernel to increase the signal-to-noise ratio. For the cerebellum analysis, warping to MNI space and smoothing occurred later. The BOLD signal in each voxel at each time point was then scaled by the mean of its respective time series to normalize the data.

The BOLD signals during the force and rest periods were modelled separately by boxcar regressors convolved with the haemodynamic response function for each task. The head motion parameters calculated during the registration step were included in the general linear model as regressors. Head motion between adjacent volumes that was greater than 0.5 mm resulted in the exclusion of both volumes from the regression analysis. Across both groups, over 94.43% of the volumes remained after excluding for head motion for both tasks. Whole-brain BOLD amplitude maps were

obtained for each experimental condition from the general linear model.

Cerebellar functional MRI preprocessing

Skull-stripped anatomical images were aligned to the SPM8 white-matter template. The transformation matrix used for this alignment was applied to the BOLD amplitude maps obtained from AFNI, thus keeping the BOLD amplitude maps consistent with the anatomical image. The cerebellum was isolated from the whole-brain anatomical image using SUIT. The isolated anatomical image of the cerebellum was then normalized to the SUIT template. The transformation matrix used for this normalization was applied to the isolated cerebellar BOLD amplitude maps. The BOLD amplitude maps were smoothed with a 4 mm full-width at half-maximum Gaussian kernel and were taken to the group level for further analysis, which was conducted using the same pipeline as the cortical data.

Functional MRI approximate entropy

To examine the time-dependent structure of the BOLD signal, approximate entropy (ApEn) was calculated on the functional MRI signal (Pincus, 1991). ApEn returns a value between 0 and 2 and it reflects the predictability of future values in a time series based on previous values. For example, a sine wave has accurate short- and long-term predictability and this corresponds to an ApEn value near 0. If varying amplitudes of white Gaussian noise are added to a sine wave, then the ApEn value would increase. This increases the uncertainty of making future time series predictions when random elements are added. For a completely random signal (i.e. white Gaussian noise), each future value in the time series is independent and not predictable from previous values, and the ApEn value tends to be towards 2. The same algorithm has been used previously on force data (Vaillancourt and Newell, 2000) and the BOLD signal in previous work (Yang *et al.*, 2013). This analysis was conducted separately for the whole-brain maps and cerebellar maps ($m = 2$; $r = 0.45 \times$ standard deviation of the signal). From this point forward, BOLD ApEn will be referred to as BOLD entropy.

Group level functional MRI analysis

The low visual feedback BOLD amplitude maps were subtracted from the high visual feedback BOLD signal amplitude maps to obtain the difference in BOLD amplitude between visual feedback levels for each individual (BOLD $\text{Amplitude}_{\text{H-L}}$). A between-group *t*-test was conducted to determine differences in BOLD $\text{Amplitude}_{\text{H-L}}$ between groups. Separate *t*-tests were conducted for the whole-brain and SUIT derived maps. Age and low visual feedback BOLD amplitude were included as covariates. The BOLD entropy maps were then subtracted between visual feedback levels (BOLD $\text{Entropy}_{\text{H-L}}$), and a between-group *t*-test was conducted to investigate differences between groups in BOLD $\text{Entropy}_{\text{H-L}}$. Similar to the BOLD $\text{Amplitude}_{\text{H-L}}$ *t*-test, age and low visual feedback BOLD entropy were included as covariates. Familywise error rate (FWER) in the group-level statistical analyses were performed in AFNI using the auto-correlation function (ACF) approach incorporated in the 3dClustSim function in AFNI, for both BOLD $\text{Amplitude}_{\text{H-L}}$ and BOLD $\text{Entropy}_{\text{H-L}}$ volumes. Results were corrected for multiple comparisons and considered significant at a corrected level of $P < 0.05$ based on the cluster size of 324 mm^3 for the cortex (ACF values: 0.71, 4.07, 11.65) and 72 mm^3 for the cerebellum (ACF values: 0.67, 4.61, 7.42). The difference in cluster size for cortex and cerebellum was due to the different smoothing factors used (8 mm versus 4 mm) in the analysis and the activation mask used in the 3dClustSim simulation. The activation mask was based upon the difference between visual feedback conditions thresholded at $P < 0.005$ for the controls.

Diffusion MRI data acquisition and preprocessing

Diffusion MRI images (repetition time: 7748 ms, echo time: 86 ms, flip angle: 90°, field of view: 224 × 224 mm, resolution: 2 mm isotropic, 64 directions, b-values: 0, 1000 s/mm^2, 75 axial slices) were collected from each participant. FSL (fsl.fmrib.ox.ac.uk) was used for all diffusion MRI data analyses (Smith *et al.*, 2004; Woolrich *et al.*, 2009; Jenkinson *et al.*, 2012). The diffusion data were first corrected for eddy currents, then for head motion using an affine registration, then the brain was extracted (Smith *et al.*, 2004). This was then used as input in two different procedures: (i) DTIFIT to calculate fractional anisotropy maps; and (ii) custom written MATLAB (R2013a, The Mathworks, Natick, MA, USA) code (Pasternak *et al.*, 2009) to calculate free water and free-water-corrected fractional anisotropy maps (FA_T), which was consistent with prior work (Pasternak *et al.*, 2009; Ofori *et al.*, 2015). To obtain a standardized space representation of the free water and FA_T maps, the original fractional anisotropy map was registered to the FMRIB FA template in standard space (1 mm isotropic) by a non-linear warp using the Advanced Normalization Tools (ANTs) package (Avants *et al.*, 2008).

Human connectome project probabilistic tractography

Tractography analyses were conducted to map the cerebello-thalamo-motor cortical pathway and several portions of the dorsal processing stream [extrastriate cortex (V3/V5) to superior parietal lobule (SPL), V3/V5 to inferior parietal lobule (IPL), SPL to primary motor cortex (M1), and IPL to M1]. We obtained diffusion weighted imaging of 100 healthy individuals from the human connectome project (HCP) database (Feinberg *et al.*, 2010; Moeller *et al.*, 2010; Setsompop *et al.*, 2012; Sotiropoulos *et al.*, 2013; Van Essen *et al.*, 2013). Diffusion images (resolution: 1.25 mm isotropic; slices: 111; field of view: 210 × 180; flip angle: 78°; b-values: 1000, 2000, and 3000 s/mm^2) were collected via a customized Siemens 3 T scanner. The HCP data were preprocessed, which included eddy current distortion correction and head motion correction (Andersson and Sotiropoulos, 2016). Probabilistic tractography was conducted using the probtrackx2 program in FSL using default settings (Behrens *et al.*, 2003; Jbabdi *et al.*, 2007). For each tract, all 100 individuals were overlapped to create a group conjunction and was thresholded at 20 subjects to create the tract template

(Archer *et al.*, 2017). These templates were then used to create slice-level FA_T and free water profiles.

Slice-level FA_T and free water profiles

Region-specific differences of FA_T and free water in each tract template were calculated using a slice-by-slice approach, which determined mean FA_T and free water in each slice of the tract along its primary axis of travel for each individual. We computed the average FA_T and free water at each slice. The average FA_T and free water was then separately compared between essential tremor patients and controls for each tract by conducting FDR corrected independent samples *t*-tests. In total, five tracts were analysed for both groups in the left and right hemispheres.

Voxel-based morphometry analysis

Data processing was performed using VBM8 toolbox (http://www.neuro.uni-jena.de/vbm/) in SPM8. Briefly, T_1-weighted images were bias corrected, tissue classified into grey matter and white matter that were normalized to a standard template using DARTEL (MNI for the cortex, SUIT for the cerebellum), modulated non-linearly, smoothed with a Gaussian kernel (8 mm for the cortex, 4 mm for the cerebellum) and input in a statistical model that evaluated differences in grey matter and white matter density between control subjects and essential tremor patients at $P < 0.05$ (FWER corrected).

Associating tremor in essential tremor with brain structure and function using multiple regression

Significant between-group functional and structural measures were used as independent variables in multiple regression analyses to determine which measures were best associated with Force $Tremor_{H\text{-}L}$ in essential tremor patients (sex and age were included as covariates). A bidirectional stepwise regression analysis was used to find the model that best described the variance in Force $Tremor_{H\text{-}L}$. The model that resulted in the lowest Akaike information criterion (AIC) was selected as the best fit model (Bozdogan, 2000). Statistical analyses were performed using the R statistical analysis package (Version 3.0.2, www.r-project.org). Multicollinearity in the resulting models was quantified using the variance inflation factor (VIF)—variables with VIF > 10 were removed. This model was then used to find the association with the FTM-TRS, Force Unfiltered $Error_{H\text{-}L}$, and Force 0-3 Hz $Error_{H\text{-}L}$.

Results

Mean force (%MVC), RMSE unfiltered (N), RMSE 0–3 Hz (N), and sum of power in the 4–12 Hz band (N^2) for the low and high visual feedback conditions are shown in Supplementary Table 1. Mean low and high dependent measures were subtracted to obtain a high-low difference measure for each individual (Force $Amplitude_{H\text{-}L}$, Unfiltered $Error_{H\text{-}L}$, 0–3 Hz $Error_{H\text{-}L}$, and $Tremor_{H\text{-}L}$); difference measures are shown in Supplementary Table 1 and Fig. 2. For mean $Force_{H\text{-}L}$ (Fig. 2A), the control group had a significantly positive score, indicating there was an increase in mean force from the low to high visual feedback condition. The essential tremor group did not have a significant change in mean force between visual feedback conditions. There was no significant between-group effect [$t(35) = 0.987$; $P = 0.33$]. Both groups had a significantly negative (Fig. 2B) Force Unfiltered $Error_{H\text{-}L}$ and Force 0–3 Hz $Error_{H\text{-}L}$ (Fig. 2C), indicating there was a reduction in force error from the low to high visual feedback condition. There was no significant between-group effect for Force 0–3 Hz $Error_{H\text{-}L}$ [$t(35) = 1.379$; $P = 0.177$] or Force Unfiltered $Error_{H\text{-}L}$ [$t(35) = 1.622$; $P = 0.114$]. For Force $Tremor_{H\text{-}L}$ (Fig. 2D), the control group did not have a significant change score; in contrast, the essential tremor group had a significantly positive Force $Tremor_{H\text{-}L}$, indicating there was an exacerbation in force tremor in the 4–12 Hz range from the low to high visual feedback condition. Furthermore, a between-group Mann-Whitney U-test found that patients with essential tremor had a significantly (U = 102.5; $P < 0.05$) higher Force $Tremor_{H\text{-}L}$ compared to controls.

Between-group differences in BOLD $Amplitude_{H\text{-}L}$

Figure 3A and B shows the significant BOLD $Amplitude_{H\text{-}L}$ for controls and essential tremor patients, respectively.

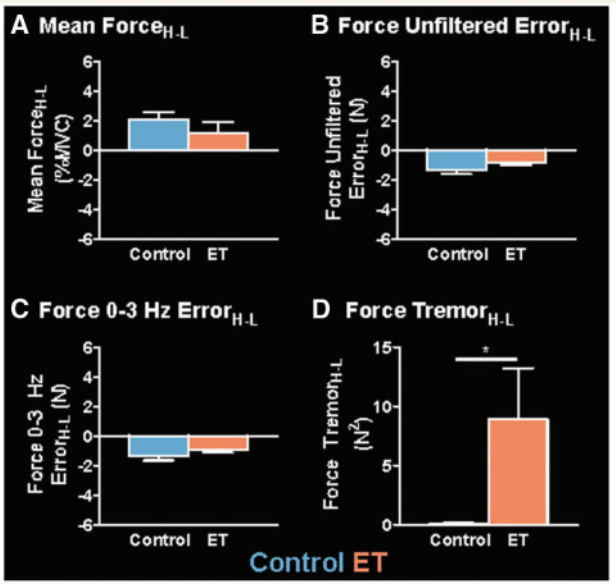

Figure 2 Group differences in mean $Force_{H\text{-}L}$, Force Unfiltered $Error_{H\text{-}L}$, Force 0–3 Hz $Error_{H\text{-}L}$, and Force $Tremor_{H\text{-}L}$. Mean values for each measure are shown for the controls (blue) and essential tremor (ET) patients (orange). Mean $Force_{H\text{-}L}$ (**A**), Force Unfiltered $Error_{H\text{-}L}$ (**B**), Force 0–3 Hz $Error_{H\text{-}L}$ (**C**), and Force $Tremor_{H\text{-}L}$ (**D**) are shown for the controls (blue) and essential tremor patients (orange). Each bar represents the group mean at each level of visual feedback, and error bars represent ±standard error of the mean (SEM). *Significant between-group differences ($P < 0.05$).

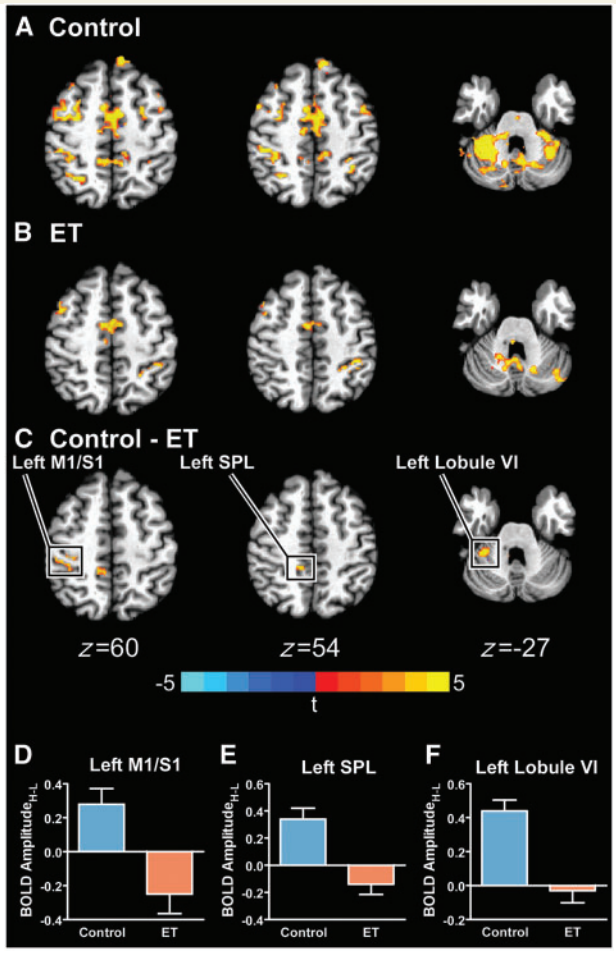

Figure 3 Between-group BOLD Amplitude$_{H\text{-}L}$ differences. The significant BOLD Amplitude$_{H\text{-}L}$ for controls (**A**), essential tremor (ET) patients (**B**), and the between-group difference ($P_{FWER} < 0.005$) (**C**) is shown. The boxed regions in **C** are plotted in **D–F**, in which the mean BOLD Amplitude$_{H\text{-}L}$ for controls (blue) and essential tremor patients (orange) is shown. Errors bars represent ± SEM.

A between-group *t*-test was conducted on the whole-brain and SUIT-derived BOLD Amplitude$_{H\text{-}L}$ maps, and revealed six clusters, which demonstrated a significant difference between groups. The centre of mass (CoM), peak *t*-statistic, volume, mean low and high BOLD amplitudes, and the BOLD Amplitude$_{H\text{-}L}$ for each cluster are shown in Table 2. Regions that demonstrated group differences in the left (i.e. contralateral) hemisphere include the primary motor and somatosensory cortex (M1/S1), SPL, IPL, cerebellar lobules I–IV, and cerebellar lobule VI. Regions that demonstrated group differences in the right (i.e. ipsilateral) hemisphere include a cluster in the lingual gyrus. All clusters showed that the essential tremor patients had a negative BOLD Amplitude$_{H\text{-}L}$ while the controls had a positive BOLD Amplitude$_{H\text{-}L}$. Figure 3C highlights the significant differences within left M1/S1 (z = 60), SPL (z = 54), and cerebellar lobule VI (z = −27). Figure 3D–F shows the

Table 2 Results of functional MRI analyses in essential tremor patients versus control subjects

	Peak *t*-statistic	CoM (MNI)			Low		High		High – Low		Effect	Volume (mm^3)
		x	*y*	*z*	Essential tremor	Control	Essential tremor	Control	Essential tremor	Control		
BOLD amplitude group differences												
Left M1/S1	3.98	−38.0	39.3	58.6	0.25 (0.30)	0.13 (0.31)	0.00 (0.46)	0.40 (0.31)	−0.25 (0.50)	0.28 (0.39)	Control > ET	702
Left SPL	4.16	−9.8	45.5	57.3	0.21 (0.33)	0.16 (0.39)	0.06 (0.39)	0.50 (0.51)	−0.14 (0.33)	0.34 (0.34)	Control > ET	486
Left IPL	3.93	−54.2	45.3	33.9	0.32 (0.42)	0.16 (0.28)	−0.13 (0.51)	0.28 (0.32)	−0.45 (0.66)	0.12 (0.36)	Control > ET	405
Right lingual gyrus	3.87	10.7	88.7	−6.5	0.28 (0.48)	0.21 (0.38)	0.11 (0.35)	0.53 (0.40)	−0.17 (0.65)	0.33 (0.42)	Control > ET	378
Left lobules I–IV	4.06	−31.0	−9.8	47.0	0.20 (0.23)	0.14 (0.21)	0.09 (0.20)	0.46 (0.28)	−0.11 (0.31)	0.31 (0.26)	Control > ET	248
Left lobule VI	4.74	−21.0	−32.8	45.1	0.18 (0.25)	0.03 (0.19)	0.16 (0.29)	0.47 (0.32)	−0.03 (0.31)	0.44 (0.27)	Control > ET	168
BOLD entropy group differences												
Right VI	−3.84	12.1	64.8	20.6	1.07 (0.26)	1.07 (0.26)	1.17 (0.24)	1.01 (0.19)	0.10 (0.12)	−0.07 (0.11)	ET > Control	376
Left SMA	−4.48	−3.0	25.0	72.6	0.97 (0.32)	0.93 (0.29)	1.12 (0.33)	0.86 (0.25)	0.14 (0.15)	−0.07 (0.19)	ET > Control	336
Right V3/V5	−4.34	25.7	76.4	38.0	1.14 (0.32)	1.02 (0.32)	1.28 (0.32)	1.00 (0.22)	0.13 (0.10)	−0.03 (0.13)	ET > Control	328

ET = essential tremor; CoM = Centre of Mass.

mean BOLD Amplitude$_{H\text{-}L}$ (±SEM) for controls (blue) and essential tremor patients (orange) for left M1/S1, SPL, and cerebellar lobule VI.

Between-group differences in BOLD Entropy$_{H\text{-}L}$

Figure 4A and B shows the significant BOLD Entropy$_{H\text{-}L}$ for controls and essential tremor patients, respectively. Identical to the BOLD Amplitude$_{H\text{-}L}$ analysis, a between-group *t*-test was conducted for BOLD Entropy$_{H\text{-}L}$. The centre of mass, peak *t*-statistic, volume, mean low and high BOLD entropy, and the BOLD Entropy$_{H\text{-}L}$ for each cluster are shown in Table 2. Regions that demonstrated group differences include the right (i.e. ipsilateral) primary visual cortex (V1), extrastriate visual areas (V3/V5), and left (i.e. contralateral) supplementary motor area (SMA). All regions showed that essential tremor patients had a positive BOLD Entropy$_{H\text{-}L}$ while the controls had a negative BOLD Entropy$_{H\text{-}L}$. Figure 4C highlights the significant differences in left SMA ($z = 71$) and right V3/V5 ($z = 35$). Figure 4D and E shows the mean BOLD Entropy$_{H\text{-}L}$ (±SEM) for controls (blue) and essential tremor patients (orange) for left SMA and right V3/V5.

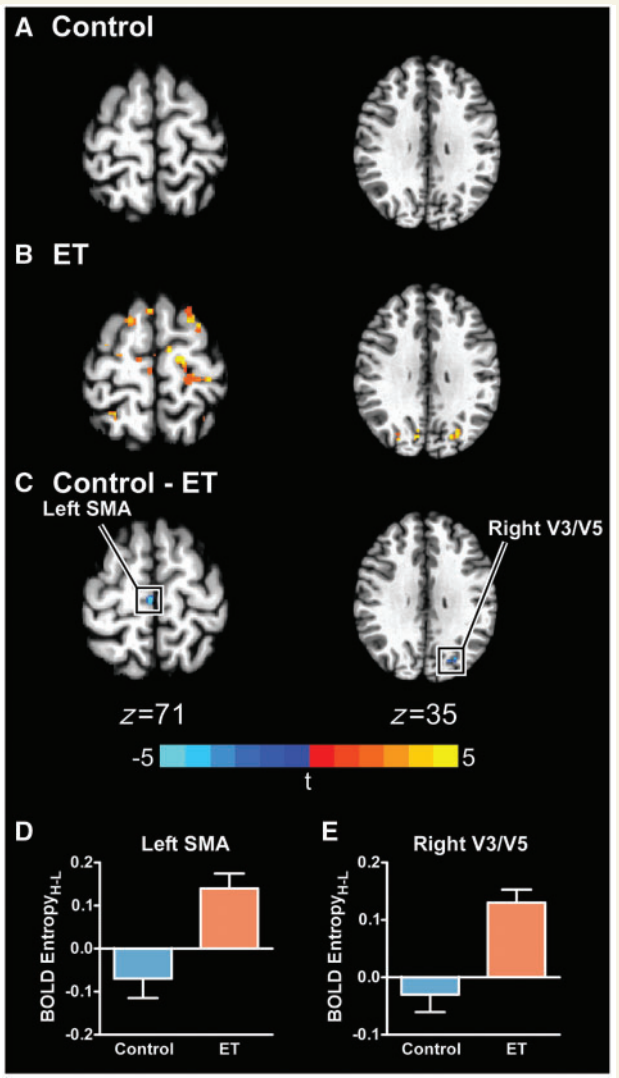

Figure 4 Between-group BOLD Entropy$_{H\text{-}L}$ differences. The significant BOLD Entropy$_{H\text{-}L}$ for controls (**A**), essential tremor (ET) patients (**B**), and the between-group difference ($P_{FWER} < 0.005$) (**C**) is shown. The boxed regions in **C** are plotted in **D** and **E**, in which the mean BOLD Entropy$_{H\text{-}L}$ for controls (blue) and essential tremor patients (orange) is shown. Errors bars represent ± SEM. SMA = supplementary motor area.

Between-group differences in FA$_T$, free water and grey/white matter volume

The cerebello-thalamo-motor cortical pathway created with probabilistic tractography is shown in Fig. 5A. The FA$_T$ slice-by-slice profile for the left and right hemispheres is shown in Fig. 5B and C, in which a black line represents the group average FA$_T$ (*y*-axis of plot) at each *z*-slice (*x*-axis of plot). Blue shading represents the ±SEM for the control group and orange shading represents the ±SEM for the essential tremor group. The cerebello-thalamo-motor cortical pathway begins at $z = -27$ in the superior cerebellar peduncle and terminates in the motor cortex at $z = 63$. The FA$_T$ along each slice varied, but no significant differences between groups were found. The free water slice-by-slice profile for the left and right hemispheres is shown in Fig. 5D and E. No significant differences between groups were found. The same analysis was conducted for several portions of the dorsal processing stream (V3/V5 to IPL, V3/V5 to SPL, SPL to M1, IPL to M1), and there were no significant differences between groups for FA$_T$ or free water. The VBM analysis also revealed no differences between essential tremor patients and controls in cortical or cerebellar grey/white matter density.

Associating tremor in essential tremor with brain structure and function using multiple regression

Significant between-group differences were found in six regions for BOLD Amplitude$_{H\text{-}L}$ and three regions for BOLD Entropy$_{H\text{-}L}$. No significant structural between-group differences were found. Therefore, the nine functional MRI regions (Table 2), as well as sex and age covariates, were used as independent variables in a multiple regression analysis to associate Force Tremor$_{H\text{-}L}$ with the BOLD signal. A bidirectional stepwise regression analysis, which minimized the Akaike information criterion (AIC) produced a significant model ($R_{adj}^2 = 42.18\%$; $P_{FDR} < 0.05$; maximum VIF = 3.33) associating Force Tremor$_{H\text{-}L}$ with BOLD signal, and included BOLD Amplitude$_{H\text{-}L}$ in left M1/S1, IPL, and cerebellar lobule VI, BOLD Entropy$_{H\text{-}L}$ in right V3/V5, and age. Figure 6A highlights these regions (BOLD Amplitude$_{H\text{-}L}$: red; BOLD

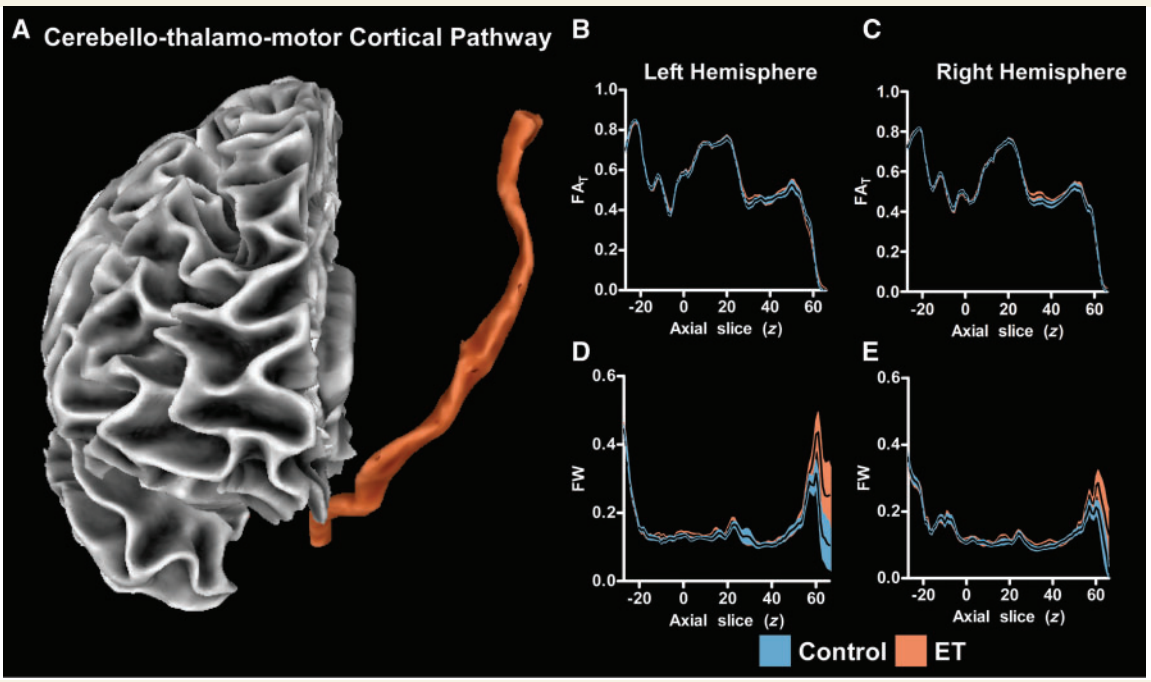

Figure 5 Probabilistic tractography FA_T and free water profiles. A 3D view of the cerebello-thalamo-motor cortical tract is shown (**A**). The FA_T profiles are shown for the left (**B**) and right (**C**) hemispheres. The mean FA_T is displayed with a black line, and the blue (control) and orange (essential tremor, ET) shaded areas represent ± SEM for each group. The free water (FW) profiles are also shown for the left (**D**) and right (**E**) hemispheres. No significant between-group differences in FA_T or free water were found.

$Entropy_{H\text{-}L}$: blue) and shows the partial regression plots for each variable, which demonstrates how each region contributes to the overall multiple regression model while controlling for all other variables. For left M1/S1, a higher BOLD $Amplitude_{H\text{-}L}$ was associated with a higher Force $Tremor_{H\text{-}L}$. In contrast, for left IPL and cerebellar lobule VI, a higher BOLD $Amplitude_{H\text{-}L}$ was associated with a lower Force $Tremor_{H\text{-}L}$. In right V3/V5, a higher BOLD $Entropy_{H\text{-}L}$ was associated with a higher Force $Tremor_{H\text{-}L}$. An increase in age was associated with a higher Force $Tremor_{H\text{-}L}$. Figure 6B (column 1) shows the actual Force $Tremor_{H\text{-}L}$ versus the predicted Force $Tremor_{H\text{-}L}$. The model significantly associating BOLD signal with Force $Tremor_{H\text{-}L}$ was also used to associate BOLD signal with the FTM-TRS (Fig. 6B, column 2) in the essential tremor patients and was significant ($R_{adj}^2 = 42.40\%$; $P_{FDR} = 0.042$). The model was also used to associate BOLD signal with Force 0-3 Hz $Error_{H\text{-}L}$ (Fig. 6B, column 3) in the essential tremor patients and was not significant ($R_{adj}^2 = 15.61\%$; $P_{FDR} = 0.761$). Moreover, an analysis using this network to predict Force Unfiltered $Error_{H\text{-}L}$ also demonstrated no significant correlation ($R_{adj}^2 = 10.50\%$; $P_{FDR} = 0.662$), indicating that this network is associated with tremor but not force error.

Discussion

The findings from the current study reveal that increases in visual feedback exacerbate the severity of tremor in essential tremor patients. This exacerbated tremor was accompanied by abnormal changes in BOLD amplitude and entropy in regions within the cerebello-thalamo-motor cortical pathway, and extended to other visual and parietal areas. Moreover, it was found that changes in BOLD amplitude (primary motor and somatosensory cortex, inferior parietal lobule, and cerebellar lobule VI) and entropy (extrastriate visual areas) were associated with changes in force tremor measured during the imaging protocol, and were also associated with clinical tremor severity. Further, this broad network was specific to the severity of tremor, but did not relate to the changes in force error induced by magnified visual feedback. This study provides direct evidence of a widespread functional network across cerebellum, motor cortex, extrastriate visual cortex, and parietal cortex associated with tremor severity in patients with essential tremor.

Essential tremor patients demonstrate an altered response to visual stimuli

While it is reasonable to propose that increases in visual feedback should increase task difficulty and therefore worsen performance on the force task, we found that increases in visual feedback error led to similar reductions in force error (Force Unfiltered $Error_{H\text{-}L}$ and Force 0-3 Hz $Error_{H\text{-}L}$) for essential tremor patients and controls. This finding, using the same visual feedback manipulation, has been consistently shown in young healthy controls,

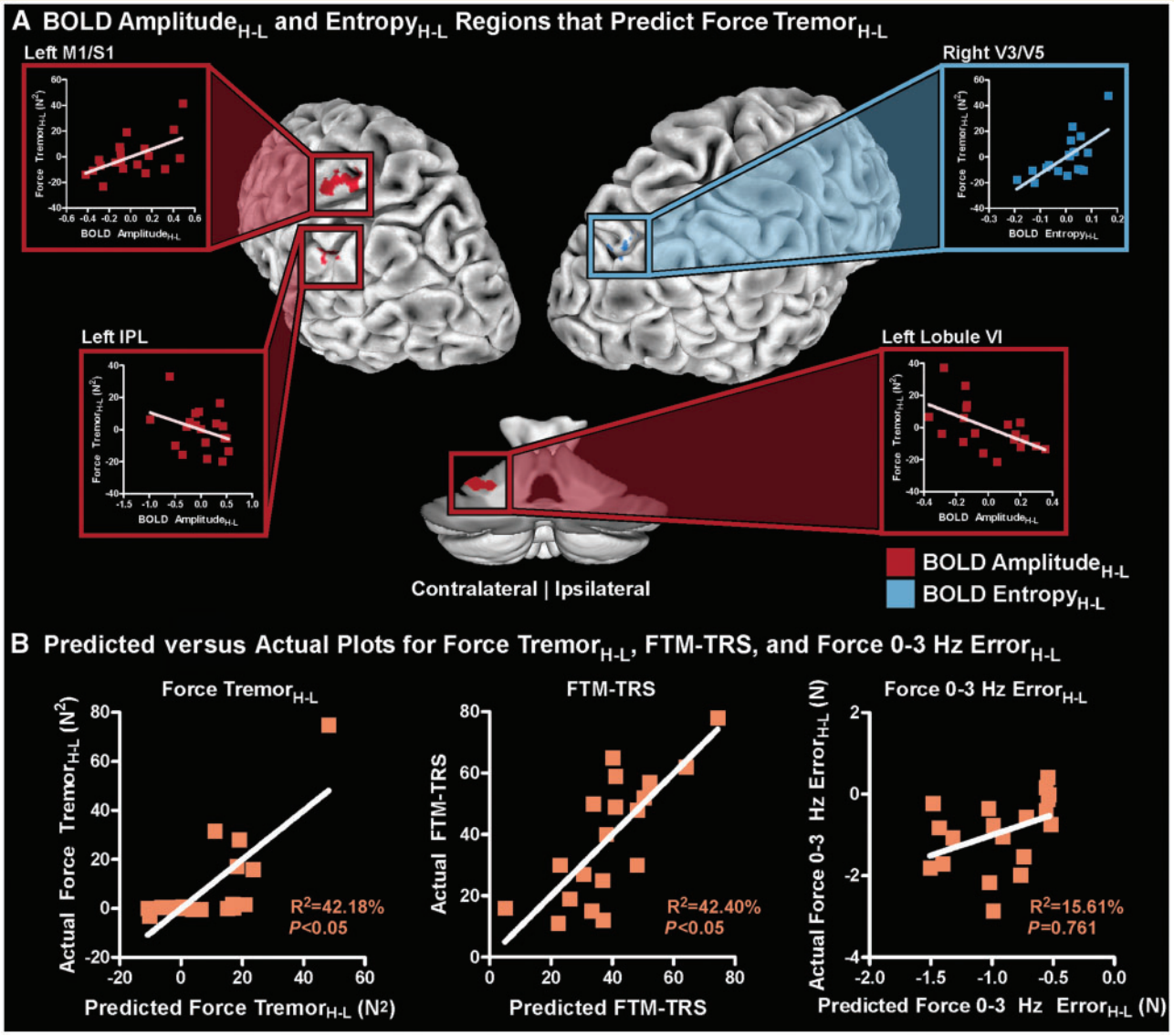

Figure 6 Multiple regression to associate Force Tremor$_{H-L}$ with BOLD signal. (**A**) The BOLD Amplitude$_{H-L}$ and Entropy$_{H-L}$ regions, which were associated with Force Tremor$_{H-L}$ includes left M1/S1, IPL, cerebellar lobule VI, and right V3/V5. BOLD Amplitude$_{H-L}$ and Entropy$_{H-L}$ regions are shown in red and blue, respectively. For each region, a partial regression plot is displayed, which shows how each region contributes to the multiple regression model while controlling for all other variables. (**B**) The predicted versus actual plots for Force Tremor$_{H-L}$, FTM-TRS, and Force 0-3 Hz Error$_{H-L}$. Age was included as a behavioural covariate.

elderly controls, and individuals post-stroke (Coombes *et al.*, 2010; Archer *et al.*, 2016). While both groups had similar changes in Force Error$_{H-L}$, there was a disproportionate increase in tremor in the 4–12 Hz range (Force Tremor$_{H-L}$) in essential tremor patients compared to controls. It has been found that the withdrawal of visual feedback in an arm extension task leads to a reduction of tremor amplitude compared to the same arm extension task in which visual feedback was provided. This finding leads to the hypothesis that increases in visual information would worsen tremor (Feys *et al.*, 2003; Keogh *et al.*, 2004), and our findings support this notion, which has long been suspected by clinicians.

Increases in visual feedback also led to an abnormal change in BOLD amplitude (BOLD Amplitude$_{H-L}$) in essential tremor patients compared to controls within, and beyond, the cerebello-thalamo-motor cortical pathway. Regions that demonstrated this finding include the primary motor and somatosensory cortices (M1/S1), SPL, IPL, lingual gyrus, cerebellar lobules I–IV, and cerebellar lobule VI. Moreover, an increase in visual feedback led to larger increases in BOLD entropy (BOLD Entropy$_{H-L}$) in essential tremor patients compared to controls in regions outside the cerebello-thalamo-motor cortical pathway, and include the primary visual cortex (V1), extrastriate visual areas (V3/V5), and supplementary motor area (SMA). Our

interpretation of this finding is that essential tremor is a network-level disorder and is not confined solely within the cerebello-thalamo-motor cortical pathway. It is possible that some of the increases in BOLD $\text{Amplitude}_{\text{H-L}}$ and BOLD $\text{Entropy}_{\text{H-L}}$ for each group in Figs 3 and 4 could be attributed to additional visual activation in the high visual feedback task; however, since both the control group and essential tremor group experienced the task at the same visual feedback levels, these visual activations would be washed out in our group comparisons. The significant regions found in this study agree with prior literature and are not restricted to visual regions. We also found that the regions that demonstrated a disproportionate change in BOLD signal were associated with the disproportionate increases in power from the 4–12 Hz and not related to force error.

The findings from the present study could provide insight into which regions should be targeted in deep brain stimulation treatment for essential tremor. Currently, deep brain stimulation is often used to circumvent the lack of an effective pharmacological treatment of essential tremor, and the current stimulation targets include the ventral intermediate nucleus (VIM) of the thalamus and the zona incerta located in the posterior subthalamic area (PSA) (Fytagoridis *et al.*, 2012; Xie *et al.*, 2012; Barbe *et al.*, 2016). The VIM thalamus has connections with the cerebello-thalamo-motor cortical pathway (Kelly and Strick, 2003), and since this pathway is implicated in essential tremor, stimulation of the VIM thalamus is often an efficient treatment of essential tremor (Fytagoridis *et al.*, 2012). Moreover, stimulation of this area has been suggested to be associated with structural changes in visuomotor areas such as V4 and V5 as well as the parahippocampal area (Tuleasca *et al.*, 2017). However, habituation of tremor suppression often occurs and the side effects can include ataxia and dysarthria (Fytagoridis *et al.*, 2012; Barbe *et al.*, 2016). The zona incerta is located in the PSA, which is located inferior to the VIM thalamus, and has connections with the cerebello-thalamo-motor cortical pathway through the basal ganglia and fields of forel (Fytagoridis *et al.*, 2012; Xie *et al.*, 2012). Tracing studies in animals show that the zona incerta has cortical connections extending from the frontal cortex to the occipital cortex (Roger and Cadusseau, 1985; Mitrofanis and Mikuletic, 1999), and also has connections to the thalamus, substantia nigra, globus pallidus, and superior colliculus (Ricardo, 1981; Power *et al.*, 1999, 2001; Mitrofanis, 2005). It is difficult to conclude if a particular stimulation target is superior in essential tremor, but it is possible that optimal targets could vary on a patient-to-patient basis. There is, however, a randomized controlled trial currently being conducted (Barbe *et al.*, 2016) that could provide more understanding in the effect stimulation target choice. This double-blinded trial will insert bilateral leads in the VIM and the PSA in 15 subjects. A crossover design will allow clinicians to evaluate the effects of stimulation in both of these regions, and determine which region induces a larger reduction in the FTM-TRS. Our results suggest that essential tremor involves a network extending beyond the cerebello-thalamo-motor cortical pathway, and therefore, a stimulation target that stimulates a more widespread functional network could be beneficial, but it is unclear whether stimulating a target with a more widespread network could also elicit more side effects.

A widespread functional network is associated with tremor

Several previous studies have associated functional MRI BOLD amplitude and connectivity with tremor in essential tremor (Buijink *et al.*, 2015; Neely *et al.*, 2015; Fang *et al.*, 2016); however, this is the first study that has shown a potential causative link between the change in visual feedback, change in BOLD signal, and change in tremor. While the present study corroborates findings of previous studies by showing that regions of the cerebello-thalamo-motor cortical pathway are associated with the severity of tremor, we extend these findings by also showing that other key regions in the visual cortex and parietal lobule are associated with the severity of force tremor and the FTM-TRS. Specifically, we found that Force $\text{Tremor}_{\text{H-L}}$ was associated with BOLD $\text{Amplitude}_{\text{H-L}}$ in the M1/S1, IPL, and cerebellar lobule VI regions and BOLD $\text{Entropy}_{\text{H-L}}$ in the extrastriate visual areas (V3/V5). Moreover, we found that while controlling for all other regions, regions within cerebello-thalamo-motor cortical pathway (M1/S1) had a different relationship with Force $\text{Tremor}_{\text{H-L}}$. Patients who had a higher BOLD $\text{Amplitude}_{\text{H-L}}$ in M1/S1 experienced a higher Force $\text{Tremor}_{\text{H-L}}$. In contrast, patients with higher BOLD $\text{Amplitude}_{\text{H-L}}$ in regions outside of this pathway (IPL and cerebellar lobule VI) experienced a lower Force $\text{Tremor}_{\text{H-L}}$. The M1/S1 and cerebellar lobule VI regions had inverse relationships with Force $\text{Tremor}_{\text{H-L}}$. Our interpretation of this relationship is that the neuronal signal travelling from the cerebellum to the thalamus is impaired, and is likely influencing the abnormal oscillations in the thalamus and cortex. BOLD $\text{Entropy}_{\text{H-L}}$ in V3/V5 correlated positively with Force $\text{Tremor}_{\text{H-L}}$. An important relationship for V3/V5, IPL, and cerebellar lobule VI is that when the changes in BOLD signal were more similar to controls, the changes in Force $\text{Tremor}_{\text{H-L}}$ were more similar to controls. We also tested to see if there was an association between the tremor network in the brain with Force Unfiltered $\text{Error}_{\text{H-L}}$ or Force 0-3 Hz $\text{Error}_{\text{H-L}}$, but there was no significant model, indicating that this network level model is specific to tremor. This is an important finding for two main reasons. First, if this network was predictive of changes in force error then this network is not specific to tremor. Second, if this network was predictive of changes in force error, then BOLD $\text{Amplitude}_{\text{H-L}}$ and BOLD $\text{Entropy}_{\text{H-L}}$ could be attributed, at least in part, to task difficulty. Since this relationship does not exist, it suggests

this network is unique to tremor. Furthermore, these regions were significantly associated with the FTM-TRS, indicating that these results are not specific to this grip force task and can be related to clinical tremor severity.

A mechanism has been described in Parkinson's disease in which there are two separate circuits associated with the amplitude of tremor and is deemed the 'dimmer-switch' model (Helmich *et al.*, 2012). In this model for tremor in Parkinson's disease, the basal ganglia plays the role of the light switch, and when the basal ganglia circuit turns 'on', it activates the cerebello-thalamo-motor cortical pathway. More activity within the cerebello-thalamo-motor cortical pathway is then associated with the amplitude of tremor, and acts as the dimmer switch in the model. It is possible that such a framework exists for essential tremor, and the current study provides new evidence that multiple regions across the cerebellum, motor cortex, visual cortex, and parietal cortex relate to changes in tremor analogous to the dimmer switch mechanism described for Parkinson's disease.

The novelty of this study is that we have found that regions outside the cerebello-thalamo-motor cortical pathway, including the extrastriate visual areas (V3/V5) and IPL, are also associated with tremor severity in essential tremor. First, we found that larger increases in V3/V5 BOLD $Entropy_{H\text{-}L}$ relate to larger increases in Force $Tremor_{H\text{-}L}$. A review paper by Vaillancourt and Newell (2002) hypothesized that an oscillating intrinsic dynamic (e.g. the BOLD signal in the grip force task used in this study) would have increased entropy in a diseased state. Our findings in this study are consistent with these predictions, and we show that increases in visual feedback can exacerbate this increased entropy, which is associated with increased tremor in essential tremor. While this is the first study to analyse BOLD signal entropy in essential tremor, other studies have used other measures. One study using resting state functional MRI in 20 patients with essential tremor found that regional homogeneity—a measurement that provides local connectivity correlations—is increased in visual areas in essential tremor patients compared to the whole-brain global average, but this does not differ from controls (Fang *et al.*, 2013). Longstanding evidence, however, has shown that the V3/V5 regions are highly involved in visuomotor processing (Paradis *et al.*, 2000; Sack *et al.*, 2006; Martinez-Trujillo *et al.*, 2007; Coombes *et al.*, 2010). Second, we found smaller increases in IPL BOLD $Amplitude_{H\text{-}L}$ led to smaller increases in Force $Tremor_{H\text{-}L}$. IPL has been implicated in visuomotor processing (Coombes *et al.*, 2010, 2011), and recent studies have associated characteristics of this region with essential tremor (Fang *et al.*, 2013; Yin *et al.*, 2016; Serrano *et al.*, 2017). A study measuring cortical thickness in IPL found that this region, in addition to the right fusiform gyrus, best diagnosed 18 essential tremor patients from 18 healthy controls (Serrano *et al.*, 2017). The IPL region used in this study was obtained from the Desikan-Killiany Atlas, which includes both IPL and V3/V5. We have built on these findings by showing that both V3/V5 BOLD entropy and IPL BOLD amplitude are associated with tremor severity. Our finding that IPL is involved in the severity of tremor is reasonable considering a recent resting state functional MRI study in 225 healthy subjects, which found that IPL has significant functional connections with M1/S1, V3/V5, and cerebellar lobule VI (Zhang and Li, 2014). Together, these findings show that M1/S1, V3/V5, IPL, and cerebellar lobule VI are all involved in the severity of tremor in essential tremor.

Structural differences in essential tremor patients

This is the first slice-by-slice probabilistic tractography analysis of the cerebello-thalamo-motor cortical and visuomotor-related tracts in essential tremor. This analysis found no significant differences in free-water-corrected fractional anisotropy (FA_T) or free water within the tracts studied, which included the cerebello-thalamo-motor cortical pathway, the primary visual cortex to parietal cortex pathways, and the parietal cortex to motor cortex pathways. There have been several region-based diffusion tensor imaging studies in essential tremor, which have shown mixed findings (Shin *et al.*, 2008; Nicoletti *et al.*, 2010; Klein *et al.*, 2011; Cerasa and Quattrone, 2016). One probabilistic tractography study of the M1-CST, SMA-CST, and M1-SMA tracts found increased FA in patients compared to controls in the SMA-CST, but no differences were found in the M1-CST or M1-SMA tracts (Gallea *et al.*, 2015). While they found differences in fractional anisotropy, it was not corrected for free water (like in the present study), which makes the measure susceptible to partial volume effects (Pasternak *et al.*, 2009). In addition to probabilistic tractography analyses, we conducted a VBM analysis of T_1 images to compare white and grey matter density between groups. We found no differences between patients and controls in the cortex or in the cerebellum. Several other studies, including the present study, have found no grey matter loss in the cortex or cerebellum (Daniels *et al.*, 2006; Quattrone *et al.*, 2008; Nicoletti *et al.*, 2010; Klein *et al.*, 2011). The lack of findings in the current study for tractography and VBM could be related to the patients included in our cohort compared with other cohorts (Daniels *et al.*, 2006; Quattrone *et al.*, 2008; Shin *et al.*, 2008; Nicoletti *et al.*, 2010; Klein *et al.*, 2011; Gallea *et al.*, 2015; Cerasa and Quattrone, 2016). It is being recognized that essential tremor may be a family of diseases with heterogeneity across individuals (Louis, 2005), and the lack of convergence across DTI and VBM studies is consistent with this hypothesis. Taken together with the functional MRI findings, this study suggests that in the essential tremor patients studied here, there are functional deficits in the absence of consistent, region-specific structural degeneration. It is important to consider,

however, that given the heterogeneity of essential tremor, these results could be specific to our cohort and tasks.

Conclusions

In conclusion, this study suggests that the tremor severity can be modulated with changes in visual feedback in essential tremor. Patients with essential tremor displayed abnormal changes in BOLD signal in regions extending beyond the cerebellum, thalamus, and motor cortex and includes the parietal cortex, primary visual cortex, supplementary motor area and extrastriate visual cortex. Further, we found that abnormal BOLD signal changes in a widespread network of regions (primary motor and somatosensory cortex, inferior parietal lobule, cerebellar lobule VI, and extrastriate visual areas) displayed a direct link with the change in the force tremor in essential tremor. Secondary analyses showed that this network was not related to changes in force error. Moreover, we show that this network is associated with clinical severity and therefore is clinical relevant. These findings support the idea that tremor in essential tremor is not driven by a single oscillator or single pathway, but is instead related to a larger network of regions.

Acknowledgements

MRI data collection was supported through the National High Magnetic Field Laboratory and obtained at the Advanced Magnetic Resonance Imaging and Spectroscopy facility in the McKnight Brain Institute of the University of Florida. Data were provided [in part] by the Human Connectome Project, WU-Minn Consortium (Principal Investigators: David Van Essen and Kamil Ugurbil; 1U54MH091657) funded by the 16 NIH Institutes and Centers that support the NIH Blueprint for Neuroscience Research; and by the McDonnell Center for Systems Neuroscience at Washington University.

Funding

This work was supported by the National Institutes of Health (R01 NS058487, R01 NS075012, K23 NS0929 57-01A1, and T32 NS082168).

Supplementary material

Supplementary material is available at *Brain* online.

References

Andersson JLR, Sotiropoulos SN. An integrated approach to correction for off-resonance effects and subject movement in diffusion MR imaging. Neuroimage 2016; 125: 1063–78.

Archer DB, Misra G, Patten C, Coombes SA. Microstructural properties of premotor pathways predict visuomotor performance in chronic stroke. Hum Brain Mapp 2016; 37: 2039–54.

Archer DB, Vaillancourt DE, Coombes SA. A template and probabilistic atlas of the human sensorimotor tracts using diffusion MRI. Cereb Cortex 2017; 1–15. doi: 10.1093/cercor/bhx066.

Avants BB, Epstein CL, Grossman M, Gee JC. Symmetric diffeomorphic image registration with cross-correlation: evaluating automated labeling of elderly and neurodegenerative brain. Med Image Anal 2008; 12: 26–41.

Barbe MT, Franklin J, Kraus D, Reker P, Dembek TA, Allert N, et al. Deep brain stimulation of the posterior subthalamic area and the thalamus in patients with essential tremor: study protocol for a randomized controlled pilot trial. Trials 2016; 17: 476.

Behrens TE, Woolrich MW, Jenkinson M, Johansen-Berg H, Nunes RG, Clare S, et al. Characterization and propagation of uncertainty in diffusion-weighted MR imaging. Magn Reson Med 2003; 50: 1077–88.

Bozdogan H. Akaike's information criterion and recent developments in information complexity. J Math Psychol 2000; 44: 62–91.

Buijink AW, van der Stouwe AM, Broersma M, Sharifi S, Groot PF, Speelman JD, et al. Motor network disruption in essential tremor: a functional and effective connectivity study. Brain 2015; 138 (Pt 10): 2934–47.

Cerasa A, Quattrone A. Linking essential tremor to the cerebellum-neuroimaging evidence. Cerebellum 2016; 15: 263–75.

Coombes SA, Corcos DM, Sprute L, Vaillancourt DE. Selective regions of the visuomotor system are related to gain-induced changes in force error. J Neurophysiol 2010; 103: 2114–23.

Coombes SA, Corcos DM, Vaillancourt DE. Spatiotemporal tuning of brain activity and force performance. Neuroimage 2011; 54: 2226–36.

Daniels C, Peller M, Wolff S, Alfke K, Witt K, Gaser C, et al. Voxel-based morphometry shows no decreases in cerebellar gray matter volume in essential tremor. Neurology 2006; 67: 1452–6.

Deuschl G, Bain P, Brin M. Consensus statement of the movement disorder society on tremor. Ad Hoc Scientific Committee. Mov Disord 1998; (13 Suppl 3): 2–23.

Deuschl G, Elble RJ. The pathophysiology of essential tremor. Neurology 2000; 54 (11 Suppl 4): S14–20.

Diedrichsen J, Balsters JH, Flavell J, Cussans E, Ramnani N. A probabilistic MR atlas of the human cerebellum. Neuroimage 2009; 46: 39–46.

Diedrichsen J, Shadmehr R. Detecting and adjusting for artifacts in fMRI time series data. Neuroimage 2005; 27: 624–34.

Elble RJ. Physiologic and essential tremor. Neurology 1986; 36: 225–31.

Elble RJ. Essential tremor frequency decreases with time. Neurology 2000; 55: 1547–51.

Elble RJ, Higgins C, Leffler K, Hughes L. Factors influencing the amplitude and frequency of essential tremor. Mov Disord 1994; 9: 589–96.

Fang W, Chen H, Wang H, Zhang H, Puneet M, Liu M, et al. Essential tremor is associated with disruption of functional connectivity in the ventral intermediate Nucleus–Motor Cortex–Cerebellum circuit. Hum Brain Mapp 2016; 37: 165–78.

Fang W, Lv F, Luo T, Cheng O, Liao W, Sheng K, et al. Abnormal regional homogeneity in patients with essential tremor revealed by resting-state functional MRI. PLoS One 2013; 8: e69199.

Feinberg DA, Moeller S, Smith SM, Auerbach E, Ramanna S, Gunther M, et al. Multiplexed echo planar imaging for sub-second whole brain FMRI and fast diffusion imaging. PLoS One 2010; 5: e15710.

Feys P, Helsen WF, Liu X, Lavrysen A, Loontjens V, Nuttin B, et al. Effect of visual information on step-tracking movements in patients with intention tremor due to multiple sclerosis. Mult Scler 2003; 9: 492–502.

Fytagoridis A, Sandvik U, Astrom M, Bergenheim T, Blomstedt P. Long term follow-up of deep brain stimulation of the caudal zona

incerta for essential tremor. J Neurol Neurosurg Psychiatry 2012; 83: 258–62.
Gallea C, Popa T, Garcia-Lorenzo D, Valabregue R, Legrand AP, Marais L, et al. Intrinsic signature of essential tremor in the cerebello-frontal network. Brain 2015; 138 (Pt 10): 2920–33.
Gironell A, Ribosa-Nogue R, Pagonabarraga J. Withdrawal of visual feedback in essential tremor. Parkinsonism Relat Disord 2012; 18: 402–3; author reply 404.
Helmich RC, Hallett M, Deuschl G, Toni I, Bloem BR. Cerebral causes and consequences of parkinsonian resting tremor: a tale of two circuits? Brain 2012; 135 (Pt 11): 3206–26.
Jbabdi S, Woolrich MW, Andersson JL, Behrens TE. A Bayesian framework for global tractography. Neuroimage 2007; 37: 116–29.
Jenkinson M, Beckmann CF, Behrens TE, Woolrich MW, Smith SM. Fsl. Neuroimage 2012; 62: 782–90.
Kelly RM, Strick PL. Cerebellar loops with motor cortex and prefrontal cortex of a nonhuman primate. J Neurosci 2003; 23: 8432–44.
Keogh J, Morrison S, Barrett R. Augmented visual feedback increases finger tremor during postural pointing. Exp Brain Res 2004; 159: 467–77.
Klein JC, Lorenz B, Kang JS, Baudrexel S, Seifried C, van de Loo S, et al. Diffusion tensor imaging of white matter involvement in essential tremor. Hum Brain Mapp 2011; 32: 896–904.
Louis ED. Essential tremor. Lancet Neurol 2005; 4: 100–10.
Martinez-Trujillo JC, Cheyne D, Gaetz W, Simine E, Tsotsos JK. Activation of area MT/V5 and the right inferior parietal cortex during the discrimination of transient direction changes in translational motion. Cereb Cortex 2007; 17: 1733–9.
Mitrofanis J. Some certainty for the "zone of uncertainty"? Exploring the function of the zona incerta. Neuroscience 2005; 130: 1–15.
Mitrofanis J, Mikuletic L. Organisation of the cortical projection to the zona incerta of the thalamus. J Comp Neurol 1999; 412: 173–85.
Moeller S, Yacoub E, Olman CA, Auerbach E, Strupp J, Harel N, et al. Multiband multislice GE-EPI at 7 tesla, with 16-fold acceleration using partial parallel imaging with application to high spatial and temporal whole-brain fMRI. Magn Reson Med 2010; 63: 1144–53.
Neely KA, Kurani AS, Shukla P, Planetta PJ, Wagle Shukla A, Goldman JG, et al. Functional brain activity relates to 0-3 and 3-8 Hz force oscillations in essential tremor. Cereb Cortex 2015; 25: 4191–202.
Nicoletti G, Manners D, Novellino F, Condino F, Malucelli E, Barbiroli B, et al. Diffusion tensor MRI changes in cerebellar structures of patients with familial essential tremor. Neurology 2010; 74: 988–94.
Ofori E, Pasternak O, Planetta PJ, Burciu R, Snyder A, Febo M, et al. Increased free water in the substantia nigra of Parkinson's disease: a single-site and multi-site study. Neurobiol Aging 2015; 36: 1097–104.
Paradis AL, Cornilleau-Peres V, Droulez J, Van De Moortele PF, Lobel E, Berthoz A, et al. Visual perception of motion and 3-D structure from motion: an fMRI study. Cereb Cortex 2000; 10: 772–83.
Pasternak O, Sochen N, Gur Y, Intrator N, Assaf Y. Free water elimination and mapping from diffusion MRI. Magn Reson Med 2009; 62: 717–30.
Peng G. Do computer skills affect worker employment? An empirical study from CPS surveys. Comput Human Behav 2017: 26–34.
Pincus SM. Approximate entropy as a measure of system complexity. Proc Natl Acad Sci U S A 1991; 88: 2297–301.
Power BD, Kolmac CI, Mitrofanis J. Evidence for a large projection from the zona incerta to the dorsal thalamus. J Comp Neurol 1999; 404: 554–65.
Power BD, Leamey CA, Mitrofanis J. Evidence for a visual subsector within the zona incerta. Vis Neurosci 2001; 18: 179–86.
Quattrone A, Cerasa A, Messina D, Nicoletti G, Hagberg GE, Lemieux L, et al. Essential head tremor is associated with cerebellar vermis atrophy: a volumetric and voxel-based morphometry MR imaging study. AJNR Am J Neuroradiol 2008; 29: 1692–7.
Ricardo JA. Efferent connections of the subthalamic region in the rat. II. The zona incerta. Brain Res 1981; 214: 43–60.
Roger M, Cadusseau J. Afferents to the zona incerta in the rat: a combined retrograde and anterograde study. J Comp Neurol 1985; 241: 480–92.
Sack AT, Kohler A, Linden DE, Goebel R, Muckli L. The temporal characteristics of motion processing in hMT/V5+: combining fMRI and neuronavigated TMS. Neuroimage 2006; 29: 1326–35.
Serrano JI, Romero JP, Castillo MDD, Rocon E, Louis ED, Benito-Leon J. A data mining approach using cortical thickness for diagnosis and characterization of essential tremor. Sci Rep 2017; 7: 2190.
Setsompop K, Gagoski BA, Polimeni JR, Witzel T, Wedeen VJ, Wald LL. Blipped-controlled aliasing in parallel imaging for simultaneous multislice echo planar imaging with reduced g-factor penalty. Magn Reson Med 2012; 67: 1210–24.
Shalaby S, Indes J, Keung B, Gottschalk CH, Machado D, Patel A, et al. Public knowledge and attitude toward essential tremor: a questionnaire survey. Front Neurol 2016; 7: 60.
Shin DH, Han BS, Kim HS, Lee PH. Diffusion tensor imaging in patients with essential tremor. AJNR Am J Neuroradiol 2008; 29: 151–3.
Smith SM, Jenkinson M, Woolrich MW, Beckmann CF, Behrens TE, Johansen-Berg H, et al. Advances in functional and structural MR image analysis and implementation as FSL. Neuroimage 2004; 23 (Suppl 1): S208–19.
Sotiropoulos SN, Moeller S, Jbabdi S, Xu J, Andersson JL, Auerbach EJ, et al. Effects of image reconstruction on fiber orientation mapping from multichannel diffusion MRI: reducing the noise floor using SENSE. Magn Reson Med 2013; 70: 1682–9.
Tuleasca C, Witjas T, Najdenovska E, Verger A, Girard N, Champoudry J, et al. Assessing the clinical outcome of Vim radiosurgery with voxel-based morphometry: visual areas are linked with tremor arrest! Acta Neurochir (Wien) 2017; 159: 2139–44.
Vaillancourt DE, Haibach PS, Newell KM. Visual angle is the critical variable mediating gain-related effects in manual control. Exp Brain Res 2006; 173: 742–50.
Vaillancourt DE, Newell KM. The dynamics of resting and postural tremor in Parkinson's disease. Clin Neurophysiol 2000; 111: 2046–56.
Vaillancourt DE, Newell KM. Changing complexity in human behavior and physiology through aging and disease. Neurobiol Aging 2002; 23: 1–11.
Vaillancourt DE, Sturman MM, Verhagen Metman L, Bakay RA, Corcos DM. Deep brain stimulation of the VIM thalamic nucleus modifies several features of essential tremor. Neurology 2003; 61: 919–25.
Van Essen DC, Smith SM, Barch DM, Behrens TE, Yacoub E, Ugurbil K, et al. The WU-Minn Human Connectome Project: an overview. Neuroimage 2013; 80: 62–79.
Whaley NR, Putzke JD, Baba Y, Wszolek ZK, Uitti RJ. Essential tremor: phenotypic expression in a clinical cohort. Parkinsonism Relat Disord 2007; 13: 333–9.
Woolrich MW, Jbabdi S, Patenaude B, Chappell M, Makni S, Behrens T, et al. Bayesian analysis of neuroimaging data in FSL. Neuroimage 2009; 45 (1 Suppl): S173–86.
Xie T, Bernard J, Warnke P. Post subthalamic area deep brain stimulation for tremors: a mini-review. Transl Neurodegener 2012; 1: 20.
Yang AC, Huang CC, Yeh HL, Liu ME, Hong CJ, Tu PC, et al. Complexity of spontaneous BOLD activity in default mode network is correlated with cognitive function in normal male elderly: a multiscale entropy analysis. Neurobiol Aging 2013; 34: 428–38.
Yin W, Lin W, Li W, Qian S, Mou X. Resting state fMRI demonstrates a disturbance of the cerebello-cortical circuit in essential tremor. Brain Topogr 2016; 29: 412–18.
Zhang S, Li CS. Functional clustering of the human inferior parietal lobule by whole-brain connectivity mapping of resting-state functional magnetic resonance imaging signals. Brain Connect 2014; 4: 53–69.